



PERGAMON

International Journal of Solids and Structures 39 (2002) 6403–6410

INTERNATIONAL JOURNAL OF
SOLIDS and
STRUCTURES

www.elsevier.com/locate/ijsolstr

Constant velocity crack propagation—dependence on remote load

K.B. Broberg

Department of Mathematical Physics, University College Dublin, Belfield, Dublin 4, Ireland

Received 5 September 2001; received in revised form 27 March 2002

Abstract

It is argued that continuum scaling applies for the dissipative region at a fast running crack edge. Then, a self-similar solution is possible for an expanding crack in a large plate. Analysis of this solution not only shows that a constant terminal velocity is reached, but also that this velocity is dependent on the remote load. However, the magnitude of this velocity may not be uniquely related to the remote load, but also dependent on features of the acceleration phase.
© 2002 Elsevier Science Ltd. All rights reserved.

Keywords: Dynamic crack propagation; Terminal crack velocity; Cell model; Continuum scaling; Fracture process region

1. Introduction

In the classical linear elastic fracture mechanics (LEFM) theory of fracture in a brittle material or in an elastic–plastic material under small scale yielding (Griffith, 1920; Orowan, 1952; Irwin, 1957), the specific energy dissipation, i.e., the dissipation per unit of crack growth, is assumed to be a material constant. This view was adopted even for dynamic crack propagation. Theory then predicted that a crack in a sufficiently large plate, subjected to remote loading, would accelerate toward the Rayleigh velocity (Broberg, 1960). However, this result could not easily be reconciled with experiments on crack propagation in glasses by e.g. Schardin (1950), showing that although a crack accelerated to a constant terminal velocity, this was distinctly lower than the Rayleigh velocity.

The vision of a velocity-independent specific energy dissipation was called in question during the 1960s, but the final blow came in the early 1970s when Paxson and Lucas (1973) determined this dissipation in PMMA to about 50 times larger at the highest crack velocity measured (about 70% of the Rayleigh velocity) than at slow crack growth. Moreover, its increase with the crack velocity was so steep that it could well indicate an unlimited rise at some velocity only slightly above the highest velocity measured. Obviously, this would explain a sub-Rayleigh terminal velocity. Further experiments, for instance by Kobayashi

E-mail address: bertram.broberg@ucd.ie (K.B. Broberg).

and Dally (1977) confirmed this by showing that the stress intensity factor continued to rise even after a constant terminal velocity had been reached.

Theoretical interpretation of the results by Paxson and Lucas had to assume an impressive increase of the size of the process region, and an explanation to this increase was given by the cell model (Broberg, 1979, 1996, 1999). A cell, which is a physically recognizable entity in the material, is in either a cohesive or a decohesive state, cf. Fig. 1, which shows a cell in a material containing particles. When the decohesive state is reached, the cell becomes unstable under load control, but a cell in situ is generally subject to a mixture of load and grip control. The process region is understood as a connected region of cells that have reached the decohesive state. At a low crack velocity, the process region is essentially confined to a single central (usually wrinkled) layer of cells. This confinement depends on the fact that after the cells in the central layer have reached the decohesive state, they impart unloading on off-side cells, which therefore are prevented from reaching the decohesive state.

At high crack velocities, communication between cells in the central layer and cells in off-side layers becomes delayed so that the information about unloading in the central layer arrives too late to prevent the cells in off-side layers to reach the decohesive state. This process may continue through several layers, and for each added layer the process region size becomes less and less dependent on the cell size. But this is effectively a loss of an intrinsic length parameter. For dimensional reasons, the presence of such a parameter is needed to explain the existence of a relation between the static fracture toughness and the crack length. For dynamic crack propagation, the effective absence of such a parameter predicts the absence of a relation between the dynamic fracture toughness and the crack velocity. Another important consequence of the effective absence of an intrinsic length parameter is, almost by definition, the applicability of continuum mechanics for a (process) region containing sufficiently many cells.

With hindsight it is realized that the absence of a unique relation between the dynamic fracture toughness and crack velocity followed already from experiments such as those by Schardin (1950) and by Kobayashi and Dally (1977), but the most compelling experimental evidence was delivered by Ravi-Chandar (1982). He found that different constant crack velocities were obtained in the same material, depending on the applied load (he used crack face loading of different magnitudes). Thus, the constant

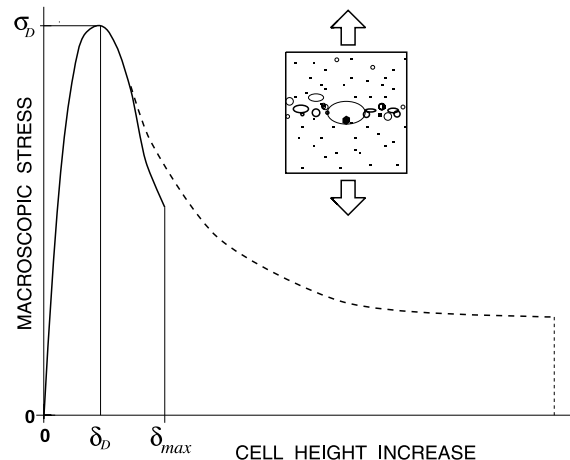


Fig. 1. Localization inside a cubic cell subjected to uniaxial loading. There is one large and several smaller particles in the element. A hole is first opened at the large particle, and after some growth of this hole, holes are opened at the smaller particles around the horizontal mid-plane. The cohesion–decohesion curve is shown by a full-drawn line. If holes are not opened at the smaller particles, the curve is modified as shown by the dashed line. σ_D is the cohesive strength, δ_D and δ_d are the elongations at which instability occurs under load control and grip control, respectively.

velocity, that had been obtained in a great number of experiments since the 1930s, could neither be considered as a material constant, nor as the maximum attainable velocity in the material.

It may be noted that constant crack velocity has been observed in two different geometrical configurations, an edge crack in a long strip subjected to fixed grip loading (this was the geometry used by Paxson and Lucas (1973)), and a central crack in a large plate subjected to constant remote loading, including equivalent configurations, such as the one used by Ravi-Chandar (1982). In both cases, the crack accelerates to a constant velocity, but the energy flux into the crack edge is predetermined for the long strip and it cannot therefore change during the constant velocity phase, as it does for crack expansion in a large plate.

2. Continuum scaling versus micro-structurally dependent scaling

The scaling laws for mechanical events in a continuum are different from those in which micro-structural processes play a part. For example, in geometrically similar beams, the plastic collapse load scales in proportion to W^2 , where W is a length dimension of the beam. On the other hand, for three point bend specimens that collapse by fracture under small scale yielding, the collapse load scales in proportion to $W^{3/2}$. It is easy to trace this difference to the fact that the size of the fracture process region at collapse load stays the same for different specimen sizes.

Similarly, continuum scaling laws do not work for a slowly moving crack. At small scale yielding, a crack starts moving when the process region reaches a certain size, independent of the crack length. Continuum scaling would have required that the linear dimensions of the process region at incipient crack growth increase in proportion to the original crack length.

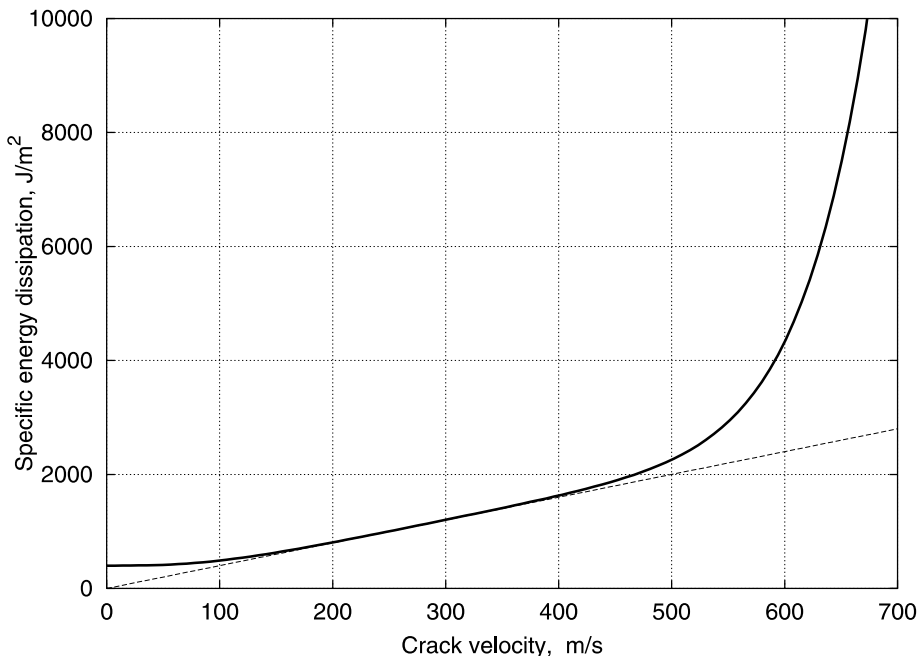


Fig. 2. Specific energy dissipation as function of the crack velocity for the long strip configuration. The curve is sketched after results by Shioya and Zhou (1995), on PMMA, extrapolated from 100 m/s to zero velocity by assuming the specific energy dissipation during slow crack growth to be 400 J/m². The dashed line shows the similarity argument approximation. The almost horizontal line for low velocities represents the minimum energy argument. The Rayleigh velocity is probably slightly higher than 900 m/s.

For a fast running crack, the situation becomes different, because, as suggested by the cell model, continuum mechanics then works even for the process region. This apparent fact was exploited in (Broberg, 1979) for consideration of fast constant velocity crack propagation in a long strip subjected to fixed grip loading. Analysis for small scale yielding lead to the “similarity argument” for a rather wide range of velocities, where the specific energy dissipation increases almost linearly with the crack velocity. One example is shown by Fig. 2.

Now, for obvious reasons, continuum scaling, and thereby the similarity argument, does not hold for arbitrarily low velocities, because that would imply crack growth under arbitrarily small specific energy dissipation. Thus, in the low velocity region, the similarity argument has to be substituted by the “minimum energy argument” (Broberg, 1979, 1999), which in the cell model corresponds to successive coalescences between the crack and cells in one single layer ahead of the crack, i.e., the minimum requirement for crack growth. The velocity, below which the similarity argument does not hold depends on the material. For PMMA it appears to be about $0.1\text{--}0.2c_R$, where c_R is the Rayleigh wave velocity, as found from results by Paxson and Lucas (1973) and Shioya and Zhou (1995).

Whereas the similarity argument may hold reasonably well for crack velocities between one third and half the Rayleigh velocity, it becomes a poor approximation for very high velocities, where the specific energy dissipation increases much more steeply than suggested by the similarity argument (see Fig. 2). There may be different reasons for this velocity dependence (Broberg, 1979, 1999). The increase with velocity of the ratio between the normal stress σ_x in the plane normal to the crack direction and the stress σ_y normal to the prospective crack plane appears to be a very important factor. In the first place, it implies a lateral constraint for decohesion, which therefore requires a larger force in the y -direction. In the second place, it affects the morphology of micro-separations, so that these are elongated in the direction normal to the crack plane, making coalescences in the crack direction more difficult, whereas coalescences normal to the crack plane lead to increasing thickness of the process region and even micro-branching.

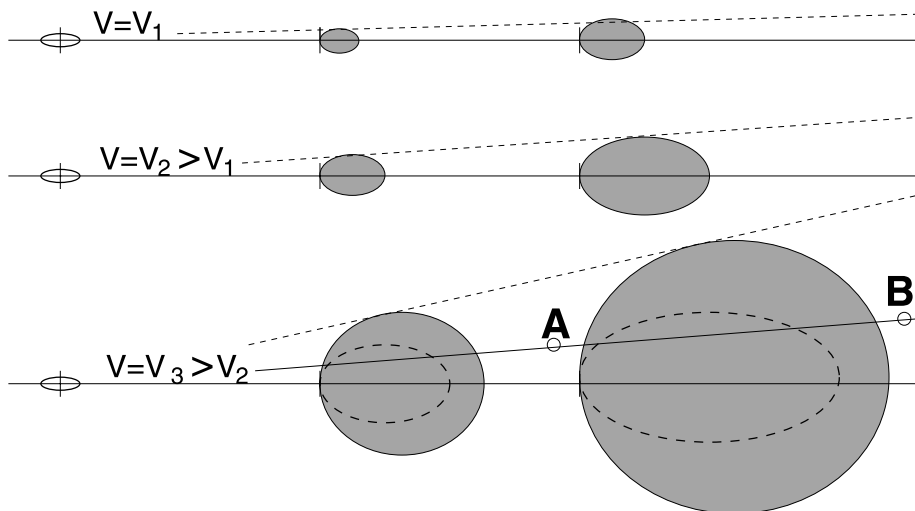


Fig. 3. Two positions of the dissipative region (shaded) during constant velocity crack expansion from a starter crack in a large plate, for three different crack velocities. Small scale yielding is assumed, but, for clarity, the dimensions of the dissipative regions are exaggerated. For velocities less than about half the Rayleigh speed, the stress field in the elastic region is fairly independent of the velocity and this is symbolized here by the similarity of the dissipative region between the two lower velocities, whereas the dissipative region takes on a different shape for the higher velocity, where the composition of the surrounding elastic field is different. For each of the three velocities, self-similarity prevails, so that material points on a straight line from the mid-point of the starter crack, for instance A and B, experience the same stress-strain history.

The typical situation for a crack in a large plate, subjected to mode I loading, is a slow crack expansion with increasing velocity under essentially constant size process region, followed by an acceleration during which the process region gradually increases, until it will be subject to continuum scaling. This leads eventually to self-similar crack expansion, i.e., constant velocity crack expansion is obtained. For high remote loads the acceleration phase may be very short (Ravi-Chandar and Knauss, 1984; Abraham et al., 1998).

Self-similar crack expansion implies that all material points on a straight line through the mid-point of the starter crack experience the same stress-strain history, except for those close to the starter crack, where acceleration effects are not negligible (see Fig. 3). Note that it is legitimate to use the concepts of stress and strain even for the process region when this behaves as a continuum. Note also the distinction between self-similarity and “the similarity argument”. Self-similarity prevails for each one separately of the three cases in Fig. 3, but the similarity argument manifests itself in the figure as a similarity between the cases with velocity V_1 and V_2 , but it is not extended to cover velocity V_3 . The dashed ovals indicate the dissipative region if the similarity argument also had prevailed for velocity V_3 .

3. A self-similar solution

Here, the case of a central crack in a large plate subjected to remote mode I loading will be discussed. It is assumed that small scale yielding prevails and that the constant velocity phase has been reached. It is also assumed that the applied load is sufficiently high to cause the crack to enter the constant-velocity phase very quickly, i.e., after a crack edge travel that is not very long compared to the length of the starter crack, and that the plate is sufficiently large to allow the constant velocity phase to prevail along a substantial distance along the crack path.

First the temporary assumption will be made that the crack velocity is not so high that the angular stress distribution in the elastic field is tangibly different from the one at low crack velocities. This would correspond to the almost linear region in Fig. 2 and the related velocity region represented by the two upper parts of Fig. 3.

Under these circumstances, simple scaling seems to apply, so that a point $(x_1, 0)$ on the path of a crack propagating with velocity V_1 will experience the same stress-strain history as a point $(x_2, 0)$, $x_2 = V_2 x_1 / V_1$ for a crack propagating at velocity V_2 . It also appears to be reasonable to assume that this stress-strain history is the same as for cracks in the long strip configuration in the velocity region where the similarity argument holds reasonably well. This would imply that the specific energy dissipation, Γ , increases in proportion to the crack velocity, V , i.e., the energy flux into the dissipative region,

$$G = \Gamma \propto Va \quad (1)$$

where a is the half-length of the crack.

Now (Broberg, 1999, p. 412),

$$G = \frac{\pi(\sigma_y^\infty)^2 a k^2 \sqrt{(1 - \beta^2)^3 R(\beta)}}{2\mu\beta^2 [g_1(\beta)]^2} \quad (2)$$

where σ_y^∞ is the remote stress, $\beta = V/c_p$ is the non-dimensional crack edge velocity, c_p is the velocity of P waves, k is the ratio between the S wave velocity and the P wave velocity, μ is the modulus of rigidity,

$$R(\beta) = 4k^3 \sqrt{(1 - \beta^2)(k^2 - \beta^2)} - (\beta^2 - 2k^2)^2$$

is the Rayleigh function, and

$$g_1(\beta) = [(1 - 4k^2)\beta^2 + 4k^4]\mathbf{K}\left(\sqrt{1 - \beta^2}\right) - \beta^{-2}[\beta^4 - 4k^2(1 + k^2)\beta^2 + 8k^4]\mathbf{E}\left(\sqrt{1 - \beta^2}\right) - 4k^2(1 - \beta^2) \\ \times \mathbf{K}\left(\sqrt{1 - \beta^2/k^2}\right) + 8k^4\beta^{-2}(1 - \beta^2)\mathbf{E}\left(\sqrt{1 - \beta^2/k^2}\right)$$

where \mathbf{K} and \mathbf{E} are the complete elliptic integrals of the first and second kind. For $\beta \rightarrow 0$, the function $R(\beta) \rightarrow 2k^2(1 - 2k^2)\beta^2$ and $g_1(\beta) \rightarrow 2k^2(1 - k^2)$.

From Eqs. (2) and (1), a relation is obtained between the constant crack velocity and the remote stress:

$$\sigma_y^\infty = \sigma_0 \frac{g_1(\beta)}{(1/\beta^2 - 1)^{3/4} \sqrt{R(\beta)}} \quad (3)$$

where σ_0 is an undetermined constant. This relation is shown by the full-drawn curve in Fig. 4, where the crack velocity is given in relation to the Rayleigh wave velocity c_R . The dashed curve is obtained by multiplying the right side of relation Eq. (1) by the ratio between the specific energy dissipation in PMMA, according to Fig. 2 and the dissipation according to the similarity argument (dashed curve in the figure). This was only done for velocities above the “minimum energy argument” region.

Constant velocity crack expansion is only obtained above some minimum velocity, say $V > V_*$. Therefore the curves in Fig. 4 are not meaningful for $V < V_*$. Judging from certain experimental results, such as

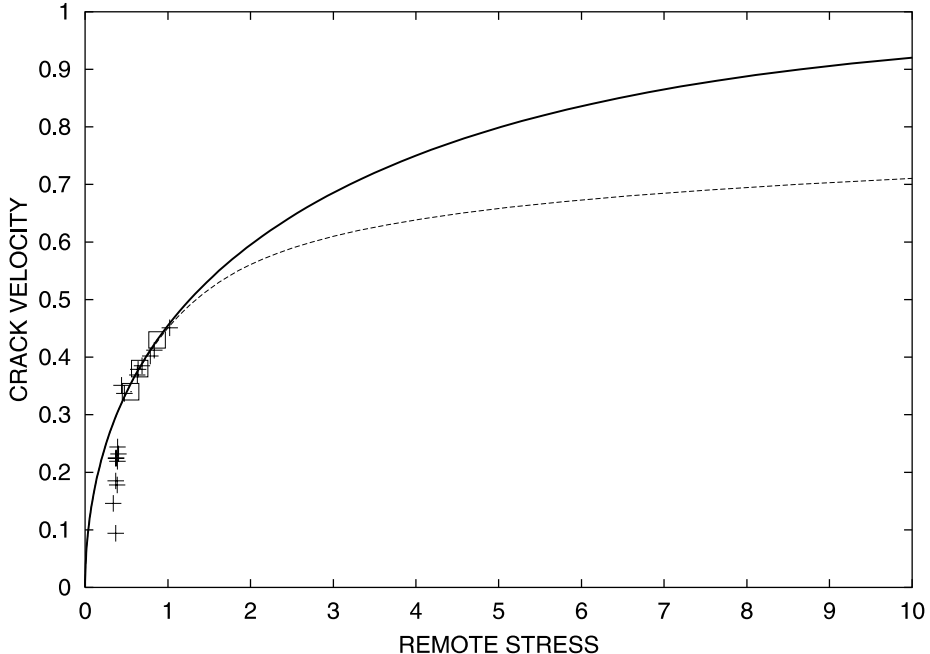


Fig. 4. Edge velocity, V/c_R , of an expanding crack, after the constant velocity phase has been reached, versus remote load, σ_y^∞/σ_0 , calculated under the assumption that the similarity argument is valid for arbitrarily high velocities (full-drawn curve). The dashed curve shows an attempt to take the deviation from the similarity argument into account. The crosses (+) and the squares (□) show data obtained from Ravi-Chandar and Knauss (1984) and Johnson (1993), respectively.

those by Ravi-Chandar and Knauss (1984), constant velocity appears possibly for $V > 0.15c_R$, where c_R is the Rayleigh wave velocity, and convincingly for $V > 0.3c_R$. Thus, V_* may be taken as a velocity between $0.15c_R$ and $0.3c_R$. These results were obtained for Homalite-100, which is similar to PMMA.

Because small scale yielding is assumed, an obvious condition is that the applied remote load must be significantly smaller than the yield stress or, in a brittle solid, the cohesive stress. This implies that the curves in Fig. 4 should be cut off beyond some maximum value of the remote stress, say around a third of the yield stress or the cohesive stress.

The constant σ_0 has to be determined from experimental results. Here, by using data on Homalite-100 from Fig. 5 in (Ravi-Chandar and Knauss, 1984), σ_0 has been chosen so that a good fit is obtained between these data for high velocities (above V_*) and the full-drawn curve in Fig. 4. Although Ravi-Chandar and Knauss used crack face loading rather than remote loading, an approximate reinterpretation to remote loading is possible.

In addition to the experimental data, results from numerical simulations by Johnson (1993), who used the cell model, have also been employed. These were given in non-dimensional form, but the remote stress was multiplied by a factor to provide a good fit. Finally, a result from a numerical simulation on silicon by Abraham et al. (1998) may be mentioned. In this simulation, a very small sample was used, subjected to an extremely high remote stress, maybe several factors of 10 higher than in typical laboratory experiments. The results obtained are very interesting from several points of view, here because the crack accelerated in a few picoseconds to a constant velocity of about $0.85c_R$, which would correspond to a point far to the right of (or beyond) Fig. 4 (note that the dashed curve, which is obtained from data for a polymer, may not be representative for a crystalline silicon).

4. Discussion

During the early, slow motion part of the acceleration phase, the specific energy dissipation in the dissipative region is essentially independent of the crack length, according to classical LEFM, and thus the scale of yielding decreases as the crack length increases. This decrease is expected to continue during the acceleration phase, although the specific energy dissipation will not stay constant but increase. After the constant velocity phase is reached, the scale of yielding will stay constant, but the specific energy dissipation will continue to increase (cf. Eq. (1)). Due to this gradual shift from constant specific energy dissipation and decreasing scale of yielding to constant scale of yielding and increasing specific energy dissipation, it may be tentatively assumed that different constant terminal velocities may be reached for the same remote load, but different acceleration. This would be a consequence of the failure to determine σ_0 except by using results from experiments on constant velocity crack expansion (but not, for instance, from constant velocity propagation in the long strip configuration). The curves shown in Fig. 4 may not be unique, i.e., another set of experimental data, perhaps with other properties of the starter crack, might lead to another estimate of the constant σ_0 .

5. Conclusion

It has been shown that a constant terminal velocity is reached for a crack expanding under small scale yielding in a large plate and also that this velocity depends on the remote load. The only assumption needed is that continuum scaling laws for rate-independent materials are applicable in the whole plate. This ought to be the case, at least approximately, for most materials of engineering interest, if the crack velocity is sufficiently high.

The constant velocity reached may not be uniquely related to the remote load. In fact, there are reasons to believe that it also depends on the history of the preceding acceleration phase. However, there does not seem to be sufficient experimental evidence available to test this hypothesis.

References

Abraham, F.F., Broughton, J.Q., Bernstein, N., Kaxiras, E., 1998. Spanning the length scales in dynamic simulation. *Computers in Physics* 12 (6), 538–546.

Broberg, K.B., 1960. The propagation of a brittle crack. *Arkiv för Fysik* 18, 159–192.

Broberg, K.B., 1979. On the behaviour of the process region at a fast running crack tip. In: Kawata, K., Shioiri, J. (Eds.), *High Velocity Deformation of Solids*. Springer-Verlag, Berlin, Heidelberg, pp. 182–194.

Broberg, K.B., 1996. The cell model of materials. *Computational Mechanics* 19, 447–452.

Broberg, K.B., 1999. *Cracks and Fracture*. Academic Press, London.

Griffith, A.A., 1920. The phenomena of rupture and flow in solids. *Philosophical Transactions of the Royal Society A (London)* 221, 163–198.

Irwin, G.R., 1957. Analysis of stresses and strains near the end of a crack traversing a plate. *Journal of Applied Mechanics* 24, 361–364.

Johnson, E., 1993. Process region influence on energy release rate and crack tip velocity during rapid crack propagation. *International Journal of Fracture* 61, 183–187.

Kobayashi, T., Dally, J.W., 1977. Relation between crack velocity and the stress intensity factor in birefringent polymers. In: Hahn, G.T., Kanninen, M.F. (Eds.), *Fast Fracture and Crack Arrest*. ASTM STP 627. American Society for Testing and Materials, pp. 257–273.

Orowan, E., 1952. Fundamentals of brittle behaviour in metals. In: Murray, W.M. (Ed.), *Fatigue and Fracture of Metals*. John Wiley, New York, pp. 139–154.

Paxson, T.L., Lucas, R.A., 1973. An experimental investigation of the velocity characteristics of a fixed boundary fracture model. In: Sih, G.C. (Ed.), *Proceedings of an International Conference on Dynamic Crack Propagation*. Noordhoff International Publishing, Leyden, pp. 415–426.

Ravi-Chandar, K., 1982. An experimental investigation into the mechanics of dynamic fracture. Ph.D. Thesis. California Institute of Technology, Pasadena, California.

Ravi-Chandar, K., Knauss, W.G., 1984. An experimental investigation into dynamic fracture: III On steady-state crack propagation and crack branching. *International Journal of Fracture* 26, 141–154.

Schardin, H., 1950. Ergebnisse der kinematographischen Untersuchung des Glasbruchvorganges. *Glastechnische Berichte* 23, 1–10; 67–79; 325–336.

Shioya, T., Zhou, F., 1995. Dynamic fracture toughness and crack propagation in brittle material. In: Kawata, K., Shioiri, J. (Eds.), *Constitutive Relation in High/Very High Strain Rates*. Springer-Verlag, Tokyo, pp. 105–112.